



MIT Open Access Articles

Flow-based fabrication: An integrated computational workflow for design and digital additive manufacturing of multifunctional heterogeneously structured objects

The MIT Faculty has made this article openly available. **Please share** how this access benefits you. Your story matters.

Citation	Duro-Royo, Jorge et al. "Flow-Based Fabrication: An Integrated Computational Workflow for Design and Digital Additive Manufacturing of Multifunctional Heterogeneously Structured Objects." <i>Computer-Aided Design</i> 69 (December 2015): 143–154 © 2015 Elsevier
As Published	http://dx.doi.org/10.1016/J.CAD.2015.05.005
Publisher	Elsevier
Version	Author's final manuscript
Citable link	http://hdl.handle.net/1721.1/112152
Terms of Use	Creative Commons Attribution-Noncommercial-NoDerivatives
Detailed Terms	http://creativecommons.org/licenses/by-nc-nd/4.0/

Flow-Based Fabrication: An Integrated Computational Workflow for Design and Digital Additive Manufacturing of Multifunctional Heterogeneously Structured Objects

Jorge Duro-Royo^{a,c}, Laia Mogas-Soldevila^{a,c}, and Neri Oxman^{b,c}

^aThese authors contributed equally to this work.

Jorge Duro-Royo: j duro@mit.edu, Laia Mogas-Soldevila: dumo@mit.edu.

^bCorresponding author: neri@mit.edu, MIT Media Lab, 75 Amherst Street, E14-433B, Cambridge, MA 02139, United States, 617.324.3626.

^cMediated Matter Group, Media Lab, School of Architecture and Urban Planning, Massachusetts Institute of Technology, 77 Massachusetts Avenue, Cambridge, MA 02139, United States.

Abstract

Structural hierarchy and material organization in design are traditionally achieved by combining discrete homogeneous parts into functional assemblies where the shape or surface is the determining factor in achieving function. In contrast, biological structures express higher levels of functionality on a finer scale through volumetric cellular constructs that are heterogeneous and complex. Despite recent advancements in additive manufacturing of functionally graded materials, the limitations associated with computational design and digital fabrication of heterogeneous materials and structures frame and limit further progress. Conventional computer-aided design tools typically contain geometric and topologic data of virtual constructs, but lack robust means to integrate material composition properties within virtual models. We present a seamless computational workflow for the design and direct digital fabrication of multi-material and multi-scale structured objects. The workflow encodes for and integrates domain-specific meta-data relating to local, regional and global feature resolution of heterogeneous material organizations. We focus on water-based materials and demonstrate our approach by additively manufacturing diverse constructs associating shape-informing variable flow rates and material properties to mesh-free geometric primitives. The proposed workflow enables virtual-to-physical control of constructs where structural, mechanical and optical gradients are achieved through a seamless design-to-fabrication tool with localized control. An enabling technology combining a robotic arm and a multi-syringe multi nozzle deposition system is presented. Proposed methodology is implemented and full-scale demonstrations are included.

Keywords: Direct Digital Manufacturing, Heterogeneous Object Modeling, Multi-Scale Feature Fabrication, Multi-Material Additive Manufacturing, Hierarchically Structured Objects, Flow-Based Computation

1. Introduction

Structures found in nature are known to display heterogeneous hierarchical materials at high strains [1]. Such functional gradients can accommodate multiple functionalities through spatial and temporal variation of material organization across length scales [1, 2, 3]. Complex physical behavior is achieved through shape-, and material-based feature and property variation of physical constituents. Advancements in digital fabrication technologies such as additive manufacturing (AM), coupled with the development of computational methods for functionally graded materials (FGM), are contributing to the development of novel multifunctional objects inspired by heterogeneous structures found in nature [4, 5, 6, 7]. The design and advanced manufacturing of heterogeneous materials and anisotropic structures spans scales and application domains from geophysical to biomedical [8], resulting in the design and manufacturing of products and systems with increased stiffness, reduced weight, wear resistance and even embedded sensing [8].

Researchers in academic institutions and industry are rapidly developing complex multi-material AM hardware posing software designers technical challenges associated with taking full advantage of hardware capabilities [9, 10, 11]. Conventional computer-aided design (CAD) tools can enable and support the manipulation of geometric and topologic virtual constructs. However, they generally lack the means to embed material data within virtual model constructs [12, 13] mostly since such tools typically assume material homogeneity [12]. The field of Heterogeneous Object Modeling (HOM) addresses the growing demands for computational tools that embed material data [14] and enable the design of functionally graded structures.

We present a customized and integrated virtual-to-physical computational workflow for the design and direct digital fabrication of multi-scale variable property objects additively manufactured using a wide range of viscous water-based materials. The workflow can encode a diverse range of interrelated multi-domain meta-data belonging to various classes of flow linking the computational tool to its digital fabrication output. Flow classes include: the flow of numeric and binary data, the flow of motion, the flow of pressure, the flow of time and the flow of water. We demonstrate the approach by assigning a wide range of material properties and extrusion geometries to basic geometric primitives in order to additively deposit heterogeneous structured constructs.

1.1. Direct Digital Manufacturing (DDM)

Direct Digital Manufacturing is generally defined as the usage of additive technologies to fabricate end-use components by digital means [11, 16]. DDM enables the generation of 3D physical objects out of 3D digital models through the deposition of material in a layer-by-layer fashion, without machining, molding or casting [15]. DDM bridges the gap between rapid prototyping and mass production, enabling the rapid manufacturing of non-standard functional and structural parts [6, 16, 17]. Many considerations and requirements come into play when considering additive manufacturing of structural parts when transitioning from Digital Prototyping to Digital Manufacturing [16]. As with the work presented here, many DDM applications take advantage of the ability of AM technologies to produce parts with geometrically complex

customized designs that cannot be mass-produced with traditional manufacturing technologies [16].

1.2. Graded Materials Additive Manufacturing

Functionally Graded Materials (FGM) are man-made materials characterized by property variation as well as high levels of anisotropic control [18]. Manufacturing processes of FGMs typically include two stages: the first involves the creation of a spatial heterogeneous structure and the second involves its consolidation [18]. Spatial heterogeneous structures are obtained with constitutive, homogenizing, and segregating methods. Spatial heterogeneous structures are obtained with constitutive, homogenizing, and segregating methods. The consolidation stage is obtained by drying, by sintering, or via solidification techniques [18]. Recent advances in automation are making both gradation and consolidation processes technologically and economically viable [17]. Within the design fields, property gradation of single materials with multiple functions carries the potential to revolutionize how products and buildings are designed and fabricated [6, 17, 19, 20, 21]. Ultimately, such advances will lead the way towards the design of multi-functional material systems with variable properties reducing the need for complex assembly of multiple parts with homogeneous properties and discrete functionality [17]. Our approach is inspired by the biological world, where single material systems are known to vary their internal composition in order to accommodate a variety of structural and environmental requirements that are then manifested in different property gradients across the surface area and volume of the manufactured product [17].

1.3. Heterogeneous Object Modeling (HOM)

Recent advancements of multi-material additive manufacturing present pressing demands on software designers to generate CAD tools that can take full advantage of novel hardware capabilities. Heterogeneous object modeling (HOM) aims at accommodating multiple objective functions within a single material construct. A heterogeneous construct is defined as an object with spatially varying material composition, as opposed to objects designed and manufactured out of a single material with constant properties [14]. Relevant work within the field of HOM was previously demonstrated that aims to better represent such constructs [12, 14, 22, 23, 24]. A range of mathematical models exists that achieve heterogeneous object representations [8, 10, 12, 14, 24, 25, 26, 27, 28]. These representations are generally classified under one of these three categories: evaluated models, unevaluated models and composite models [14]. Strategies known to encode material distributions in such methods are: (1) discretization of the objects volume into simple *parameterizable* elements, (2) implement a simple parameterization whose domain does not coincide with the objects boundaries, or;(3) construct a specific parameterization for the interior and boundary of each object [29, 14].

The main issues with the virtual representations of material anisotropy are associated with the difficulty in parameterizing the interior of a given boundary representation of a solid model [29]. Researchers have developed computationally efficient solutions to represent heterogeneous objects in the realm of computer graphics and animation [41, 42] that use mesh-free geometry such as implicit surface primitives [41], or interpolated scalar fields onto surfaces of primitives defined as diffusion surfaces

[42]. Since typical 3D printing software is designed to assign single materials per polygon meshes representing the object, any continuous gradation between multiple materials raises technical challenges. These challenges appear again when material properties and geometrical features are decoupled, and custom material definitions that are not embedded in the system are reused [13].

The proposed workflow associates heterogeneous material properties to mesh-free geometric primitives like curve trajectories in order to improve heterogeneous object fabrication. We calculate and incorporate meta-data parameters such as speed, pressure, or time delays into machine code communicated to the fabrication platform. We address the design and representation limitations of heterogeneous objects by continuously controlling material organization and variable extrusion geometries through time-dependent flow functions, and by establishing an extendable calibrated material database with deposition-related parameters stored within the software. Continuous control is based on accurate synchronization of a positioning platform (e.g. a robotic arm) and a deposition platform (e.g. a multi-chamber pneumatic extruder attached to the arms end-effector) (Figure 1). This synchronization enables controlled flow and speed variation along deposited paths. In addition, it enables sectional height and overall thickness variation of multi-material extruded geometries.

1.4. Integrated Design-to-Fabrication Systems

File-to-factory design approaches provide the ability to merge Computer-aided Design (CAD), Computer-aided Engineering (CAE) and Computer-aided Manufacturing (CAM) into a single seamless digital process [30, 31, 32]. It involves the transfer of data from 3D-modeling software environments to a CNC (Computer Numerical Control) subtractive or additive digital fabrication platform [33, 34]. In most cases the data transfer process implies the translation of the virtual design into the G programming language (known as “G-code”) for controlling automated machine tools defining optimized tool paths and operating speeds [35]. This is commonly achieved by exporting the virtual design using a specific file format and reopening this file using the CNC tool software environment installed by the manufacturer [36]. Following, material dimensions and tool paths are assigned with limited possibility for further iterations as well as incompatibilities between the original software environment and the G-code that are lost in translation. Such discrete and streamlined tool-based process is all but seamless, framing and limiting the workflow of designs that are complex in shape and heterogeneous in material composition.

Architectural and design firms with particular interest in direct digital manufacturing of non-standard building parts are in need of workflows that fuse computational modeling environments with manufacturing platforms [37]. As a result some establish common online databases that are accessible to the manufacturer, or that embed instructions in the fabrication file itself in order to secure the most appropriate method for realizing their parts [33]. Furthermore, relying on unprecedented degrees of mechanical precision DDM designs in product and architectural scales are defined by zero tolerance between virtually defined features. In order to ensure accuracies of sub-millimeter length scales of products and architectural parts, new DDM tools and their respective software environments must strive towards high definition manufacturing as can be found in the automotive and aeronautic industries [34]. Large-scale high-definition

(LSHD) fabrication requires the generation of irreducible representations across domains including geometrical features and material properties [34].

Our proposed workflow and LSHD DDM system aims to integrate design and digital fabrication environments by way of calibrating metadata defining the flow of bits and atoms in a continuous fashion starting with original geometrical intentions and ending with the manufactured construct. Meta-data available to the system is comprised of product definitions (geometric, topologic and material specifications) as well as process definitions relating to mechanical deposition and spatial positioning constraints. In order to access, process, interpret and interrogate the vast quantity of data, multiple domain methods are implemented as described in Section 3 of this paper. We coined the term Flow-Based Fabrication to refer to the meta-data manifold.

2. Materials and Methods

2.1. Software

Geometric objects and tool paths presented in this paper were designed within the Rhino3D modeling software environment (2013, Rhinoceros, Robert McNeel and Associates, USA) and its scripting plugin, Grasshopper [38]. Using the geometric kernel library of the plugin, custom C-sharp code was written to transmit fabrication XML instructions to a central interface. The communication applet was written in C++ using the Qt open-source platform (2014, Qt project, Norway). The applet processes input and output data generated in the design platform to and from mechanical parts. Transmission to the motion system is achieved via an Ethernet UDP socket, and to the extrusion system - via a serial USB signal. The pneumatic tool firmware was developed in C code using the Eclipse IDE environment (2014, The Eclipse Foundation, Canada) and the cross-platform open-source Arduino library (2014, Arduino Software, Italy).

2.2. Hardware

A Mastech Linear DC power supply, model 30V 5A HY3005F-3, with triple outputs and dual adjustable outputs (0-30V and 0-5A) was used to power pneumatic hardware components for positive and negative pressure at 25V and 0.6A. The system's control board is an Arduino Mega 2560, with a computer supplied input power of 5V and an output power of 3.3V or 5V, incorporating a high performance, low power Atmel AVR 8-Bit micro-controller. An eight-channel 5V relay shield module for Arduino (SunFounder brand) was mounted on the microcontroller and connected to positive and negative pressures. Pressure is controlled by directional solenoid valves with a 3-way, 2-position, normally closed spring return poppet valve with aluminum stackable body. Other valve specification include: 1/8 inch NPT female ports, $C_v=0.051$, 24VDC single solenoid, 11mm DIN style wiring connector, and a minimum response time of 0.05s, which we take into account in our computation sequence. Pressure is tuned with a compact size general-purpose electronic pressure regulator, converting a 4 to 20 mA signal to a proportional pneumatic output (ranging from 0 to 120PSI) with a sensitivity of 2.5% of span per PSI (OMEGA IP610-X120). We included a 1s response time for the regulator. Signal to the regulator is computed through a low-power high-accuracy single channel, 12-bit buffered voltage output Digital-to-Analog Convertor (DAC) board with non-volatile memory (MCP4725 Board). Output pressure from the regulator is read with

a ProSense digital pneumatic pressure transmitter, with a -14.5 to 14.5 psi range, 2 PNP, 4- 20 mA, 1/8 inch NPT outer pressure connection, M5 inner pressure connection, powered by 12-24 VDC. The hardware assembly detailed here is illustrated in Figure 3a.

2.3. Mechanical Assembly

The extrusion system is attached to an existing motion platform's end-effector. The platform is a Kuka KR AGILUS robotic arm; model KR 10 R1100 SIXX WP. It weighs 54kg with a 10kg payload and a maximum reach of 1101mm. It has 6 axes, a ± 0.03 mm repeatability and employs the KR C4 compact control system. At the pneumatic extrusion end-effector, different materials are contained in six 300cc clear plastic dispensing syringe barrels with hard rubber plungers, and extruded with 7mm and 2mm customized HDPE plastic nozzles. Flow valves, gauges and tubing are dimensioned to 4mm 10PSI to 120PSI pneumatic circuitry. Positive pressure is obtained with a 4.6 gallon aluminum twin-tank air compressor with 1.5 horsepower, 120 volts, 60 Hz 4.2 CFM at 90 PSI and 5.4 CFM at 40 PSI. Negative pressure is obtained with a rotary vacuum pump at 1725 RMP and 110 volts, 60 Hz. For the mounting of the custom end-effector parts we used 5mm and 10mm machinable aluminum sheets cut with a numeric control abrasive water-jet machine (OMAX Corporation, USA). These mechanical assembly parts are illustrated in Figure 3b.

2.4. Deposition Materials

The multi-material pneumatic deposition tool-head that we developed is able to extrude materials with viscosities ranging from 500cPs to 50,000cPs at room temperature such as; hydrogels, gel-based composites, certain types of clays, organic pastes, resins, polyvinyl alcohols etc. In the experiments presented here we used polysaccharide hydrogels in 1% to 12% concentrations in w/v of 1% acetic acid aqueous solutions, as well as these gels mixed with cellulose microfiber to obtain volumetric composites. Their testing, characterization and processing are explained in detail in our previous publication [17] and in our patent [39]. The materials present visco-plastic or visco-elastic behaviors inside airtight barrels and undergo slow curing from pastes to solids at room temperature. Exhaustive empirical testing of these materials and their combinations is stored in the platform's database to inform calculations of the model's parameters for pneumatic deposition and positioning motion. Other synthetic materials such as fuse deposition manufacturing (FDM) polymers can be used as well, by implementing heating nozzles, as material and tool settings are externalized from the core computation.

3. Flow-Based Fabrication: Computational Workflow for Design and Direct Additive Manufacturing of Multifunctional Heterogeneously Structured Objects

We present a model, an enabling technology and a workflow sufficiently generalized to adapt to a wide range of materials and digital fabrication platforms [39]. The proposed workflow is designed to integrate the virtual modeling environment to the physical fabrication platform, achieving multi-material and multi-property constructs at the service of multi-functional objects (Figure 1). We propose that seamless computational workflows such as the one presented here, can be viewed as vehicles to encode multidisciplinary non-standard design constraints into generative frameworks.

These frameworks can provide for methodological design tools that enable navigation between tightly related constraints typical of complex and heterogeneous designs.

Every flow layer included in our system is independently defined. Importantly, 3D constructs characterized by complex material organization will emerge, not by direct 3D modeling, but by meta-data instructions informing the manufacturing process through variable motion speed, variable pressures and diverse water-based viscous material compositions. These interrelated processes can be rationalized through domain-specific flow fields. Flow fields include the flow of data (section 3.1), the flow of bits (section 3.2), the flow of motion (section 3.3), the flow of pressure (section 3.4), the flow of time (section 3.5), and the flow of water (section 3.6).

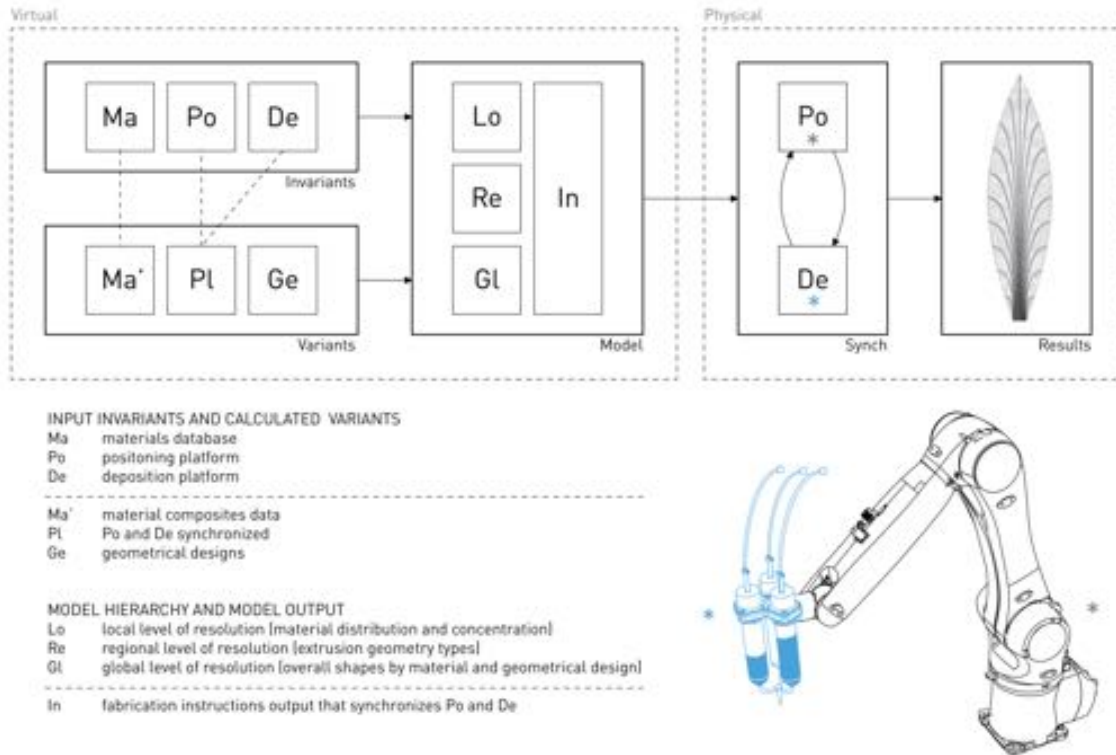


FIGURE 1: Overview of our computational workflow for design and direct additive manufacturing of heterogeneously structured objects. Virtual hierarchical computation is implemented at local (Lo), regional (Re) and global (Go) levels of organization. It combines variants and invariants given by base materials (Ma) and their combinations (Ma'), the positioning platform (Po), the deposition platform (De) and the geometrical design (Ge). The model generates fabrication instructions (In) that are transmitted in synchrony to both platforms (Pl). Heterogeneous structured results are obtained from this seamless virtual-to-physical workflow. As an example, a positioning platform (Po) is depicted as a 6-axes robotic arm and a deposition platform (De) is depicted as a three-barrel pneumatic extruder.

3.1. The Flow of Data

The flow of data is initiated by variant design parameters and invariant system constraints defined by the system's building blocks. These include: the materials to be extruded (Ma, Ma'), the positioning platform (Po), the deposition platform (De), and the geometrical designs (Ge) (Figure 1). The system is defined in a way that is as general as possible by variant and invariant constraint parameters independent and external to the hardware system in use. The goal is to enable its implementation using various DDM platforms. In the current testing system a positioning platform (Po) is given as a 6-axis

robotic arm, and a deposition platform (De) is given as a multi-barrel pneumatic extruder (Figure 1, Figure 3).

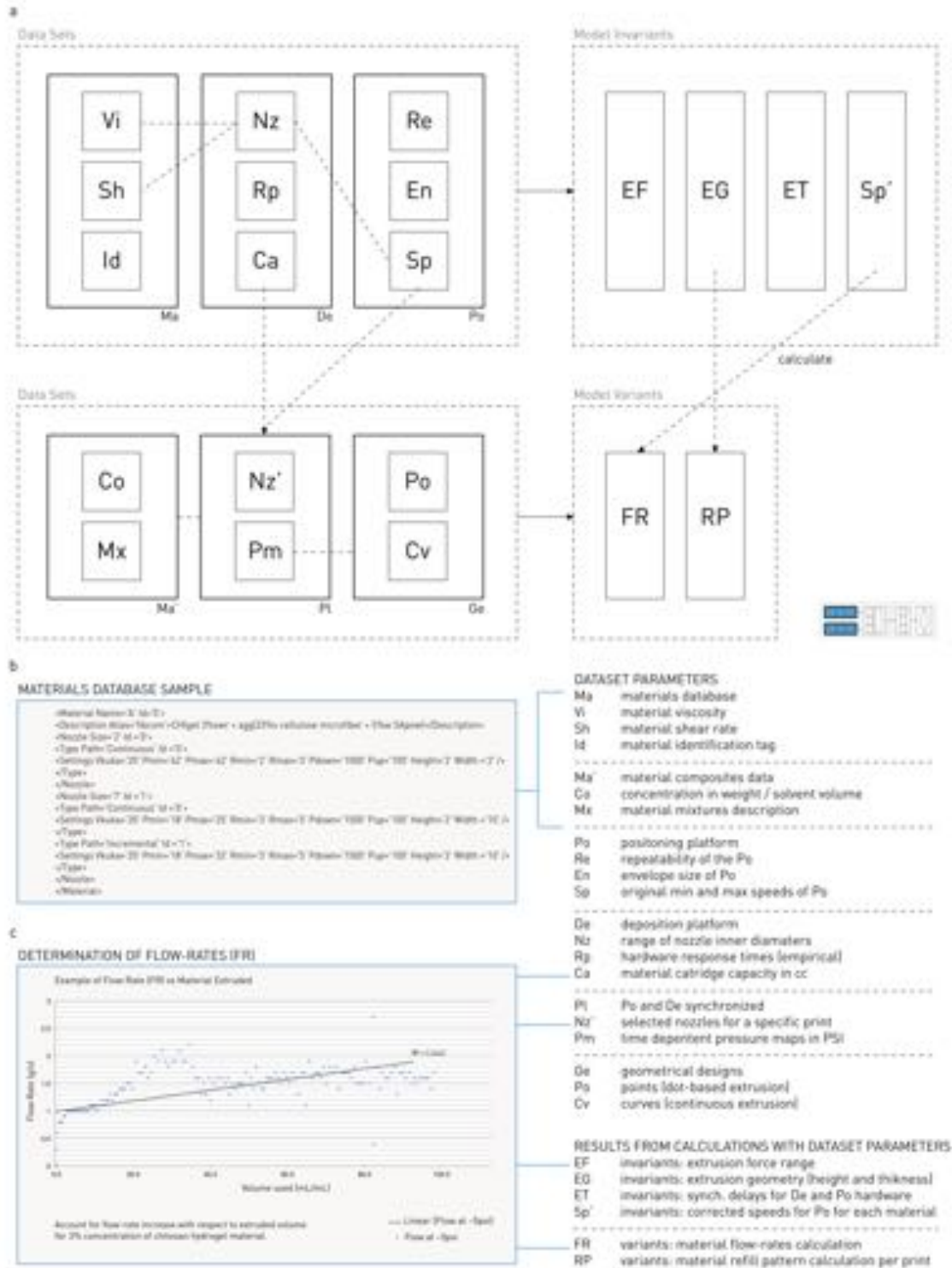


FIGURE 2: (a) Data including materials (Ma, Ma'), platform parameters (Po, De, Pl), and geometrical design (Ge), is incorporated within the computational model. Processing of this data into calculations results in global constants (invariants) and design specific parameters (variants). The model invariants compute the range of extrusion forces (EF), the height and thickness ranges of the extrusion geometries (EG), the extrusion delays and synchronization timings

required (ET), and the corrected speeds of the positioning platform (Sp'). The model variants compute the required flow-rates (FR), and the pattern of barrel refills over time (RP). (b) A sample of the materials database. Empirically tested material specific parameters such as minimum and maximum extrusion pressure, nozzle height, hardware delays, and motion speed are stored and used for the calculation of code variants. (c) We add corrections to our extrusion pressure calculation by determining the linear increase of flow-rate due to cartridge level changes over time.

3.1.1. Invariants

Invariant constraints serve to calculate the platform-specific constant parameters of the system. Parameters related to base materials (Ma) include: viscosity (Vi), shear rate (Sh) and material identification (Id). We calculate the invariant constraints of the deposition platform (De) through: range of nozzle types (Nz), hardware response times (Rp), and material reservoirs capacity (Ca) (refer to Section 2.2 for further detail). Previous research into nozzle designs can be found in [17] (Figure 2a).

Finally, the invariant constraints of the positioning platform (Po) are calculated using: system repeatability (Re), envelope size (En), as well as minimum and maximum speeds (Sp). With the mentioned sets of parameters, the system can calculate the invariants which are: range of extrusion forces (EF) required for a given design, the range of extrusion 3D-shapes to be deposited (EG), the range of extrusion timings and delays, and the revised speeds (Sp') of the positioning platform (Figure 2a).

3.1.2. Variants

Variant constraints serve to calculate specific parameters of the computation that change at every design. They relate to parameters from the selection and combination of base materials (Ma) into composites (Ma'); degree of concentration of material in solvent (Co), and description of the composite characterization for further reference and testing (Mx) (Figure 2b). A calibration capability can be used such that, in addition to the set of initial materials (Ma), an extendable database of material behavior is stored as different materials are tested by the system. This practice allows for platform and workflow validation at step of the development process.

Other platform parameters available that contribute to variant calculation include: nozzle type chosen (Nz') e.g. to perform co-axial, parallel or mixed extrusions as well as time-dependent pressure maps (Pm) that determine the extrusion geometry (see Section 3.1.4). Hardware response times (Rp) are calculated empirically and inform the calculations, as well as the measurements of the cartridge capacity (Ca). Continuous, discontinuous or discrete geometries, such as points (Po) or curves (Cv) can be assigned with the aforementioned material choices and time-dependent pressure maps. With the mentioned sets of parameters, the system is designed to calculate the range of variant flow-rates (FR) required for a particular multi-material design, and patterns of reservoir refill over time (RP) (Figure 2a).

The extrusion shape map is defined per material and includes the extruded volume per n map repetition along a given trajectory. As a result, each extrusion length map Lt is compared to a control extrusion length Lc associated with a typical continuous extrusion. In order to determine the refill pattern of the material barrels (RP) we compute:

$$Lc = \sum_{i=1}^n Lt \times cs \times ct, \text{ where } cs \text{ is an estimate security coefficient (0.75) and } ct \text{ is the}$$

averaged type of extrusion map that the trajectory carries. It is assigned the value of 1.00 for continuous paths and 0.25 to 0.75 for discontinuous ones.

Flow rate (FR) calculations inform the pressure maps for each extrusion and a given material. Figure 2c illustrates the calibration of the platform with 3% concentrated chitosan polysaccharide hydrogel material. Linear flow resulting from the relationship between flow rate and material already extruded out of the barrel can be defined by $y=0.01x+1$. This account is calculated for each material in the Ma and Ma' databases and used to correct the flow rate (FR) along the print job and over time.

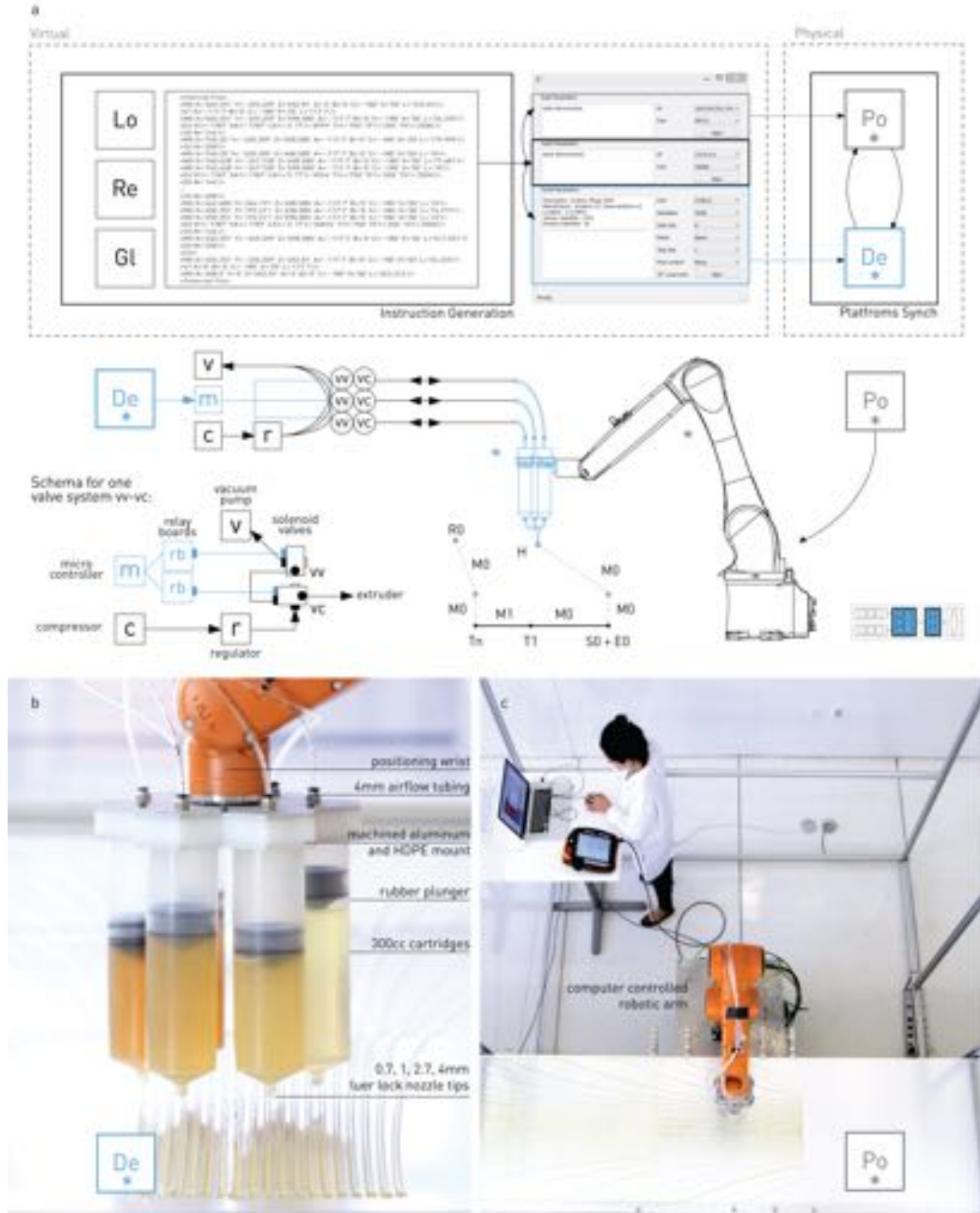


FIGURE 3: (a) The virtual model operates at three levels of resolution; local (Lo), regional (Re) and global (Gl) to fabricate heterogeneous structured objects. These hierarchical computation results are converted to fabrication instructions that are fed to a distribution interface that coordinates both positioning (Po) and deposition (De) platforms. The physical construct is achieved by implementing pressure (v,c,r), electrical (m), extrusion (E0) and motion (M0, M1, S0, R0, T1, Tn) data flows that tightly link both platforms. (b) In an exemplar application of the presented framework, a 6-barrel multi-material deposition system (De) is custom designed, built and attached to a robotic arm. (c) The computer-controlled robotic arm acts as the positioning system (Po) and receives instructions from the distribution interface in synchrony with the deposition system (De).

3.1.3. Instructions

Once the variant and invariant parameters are calculated, local (Lo), regional (Re) and global (Gl) strategies for material heterogeneity (Figure 4, 5, 6) are implemented to structure the geometrical construct. The instruction data containing nozzle heights, time delays, and pressure maps to achieve such hierarchy is computed via Extensible Markup Language (XML) and transmitted to an instruction interface that will distribute it to both positioning (Po) and deposition (De) platforms (Figure 3a). The interface is designed to distribute instructions while taking into account constraints of both platforms in order to synchronize motion and extrusion for complex depositions.

3.2. The Flow of Bits

The flow of bits is initiated within a design-modeling platform and transitions to the deposition platform via serial USB communication. The deposition system (De) is located at the positioning system's (Po) end-effector and is based on a multi-barrel head digitally actuated by pneumatic hardware and circuitry. Bits flow from a micro controller (m) into relay boards (rb) that control solenoid valves (vv and vc) connected to a vacuum pump (v) and a pressure regulator (r) that receives a constant supply of airflow from an air compressor (c). Each vc valve outputs pressure to a given material barrel. Pressure levels enable start and stop deposition with positive and negative pressure respectively (Figure 3a). The pressure regulator (r) transforms the flow of bits into flow of pressure and receives variable impulses that determine different regional extrusion geometries with tunable heights and widths along the trajectory (Figure 5a). We empirically calibrate the regulator's pressure response (P) when given input values from 0 to 4000 of type 16-bit unsigned integer, that correspond to 4 to 20mA of electrical current (I). A linear interpolation is then performed as follows; $I = I0 + (I1 - I0) * (P - P0 / P1 - P0)$, so that the flow of pressure is mapped onto the flow of bits.

3.3. The Flow of Motion

Motion flow is transmitted from the instruction interface via an Ethernet UDP socket to the positioning platform every 0.012s. The positioning platform is instructed to follow complex paths made of points, lines, poly-lines or curves through different motion instructions, starting from a point in space called home (H). The motion types can be M0 (composed of multiple targets), M1 (composed of a single target), S0 (a static motion), and R0 (a reservoir refill motion) (Figure 3). The M0 motion spans the first trajectory target (T1), and carries the total length of the trajectory ensuring smooth positioning even if the trajectory is composed of multiple targets (Tn). A static motion S0 carries the amount of instruction cycles in order for the system to remain static. This avoids repetition of identical instructions to be sent, and therefore makes the allocation less computationally intensive, as the internal instruction file is substantially reduced in size.

A refill motion R0 targets the same custom point in space and awaits for user action indicating that the reservoir, or reservoirs, are refilled properly and further action can take place (Figure 3).

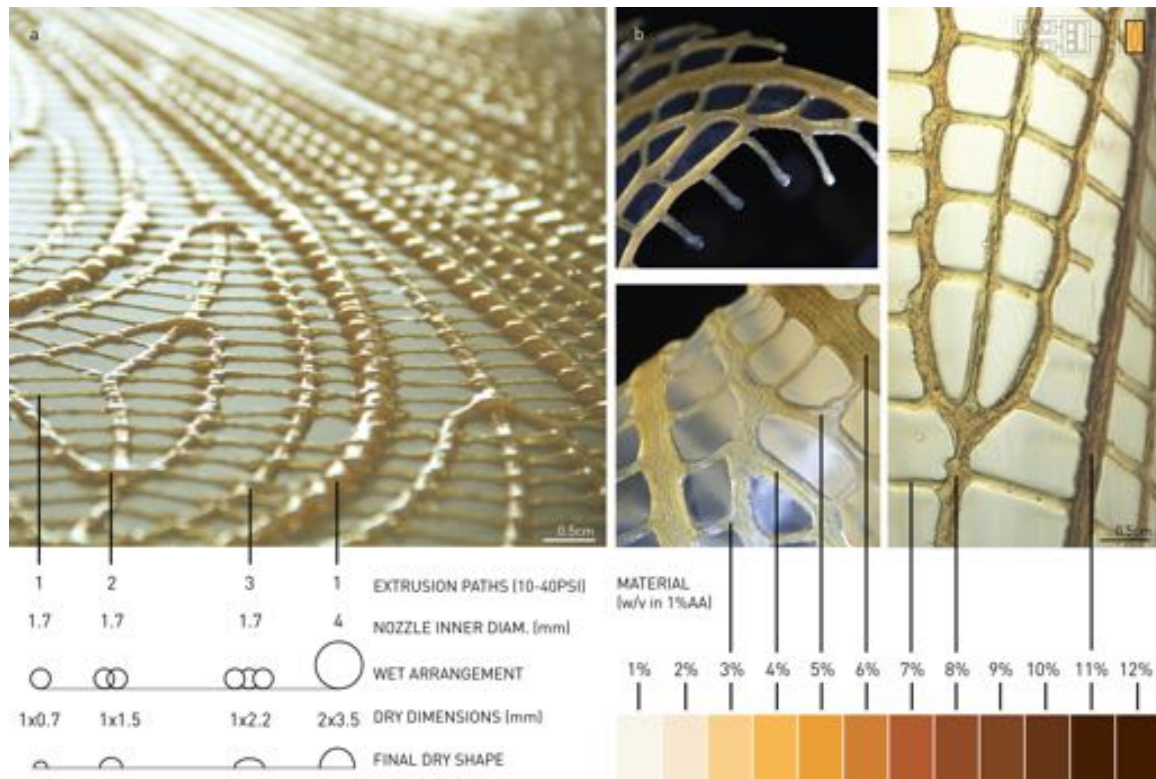


FIGURE 4: (a) An example deposition is analyzed to demonstrate material distribution patterns in cross section and resulting dry constructs. The material used in this example is an hydrogel, consequently, the volume of the deposition is significantly reduced after curing. (b) Different concentrations of polysaccharide hydrogel in mild acidic solutions can be employed to generate a gradient of materials with different opacities, viscosities and stiffness's.

3.4. The Flow of Pressure

Each extrusion path is designed such that it can define different extrusion shapes and material properties from base materials (Ma) or from new combinations of base materials (Ma'). This is due to the fact basic curve primitives (Figure 5b) are assigned material properties in the model as opposed to processes, which take as input polygonal meshes. The flow of motion and pressure can vary while following the primitives providing different speeds, extrusion forces, and material volumes from each reservoir. From a positive pressure source (air compressor, c) and a negative pressure source (vacuum pump, v) airflow is transmitted into the system's valves in order to deposit materials in different levels of organization (Figure 3a). At the local level, different materials in different concentrations, and diverse layering strategies can be assigned to distribute material along trajectories. Figure 4a demonstrates different layering deposition strategies providing structural hierarchy within the construct. A gradient of local stiffness given by material concentration (1% to 12% in aqueous solution) is depicted in Figure 4b and its instances identified in a dried construct. Regional levels of control are achieved by differentiating extrusion geometries in height and width through pressure and motion

flow maps. The regional pressure flow is described by three main classes (Figure 5d): a data allocator is in charge of reading the motion and deposition instructions (A_t) at the beginning of each complex path, taking around 5ms. Then a regulator sets the initial pressure (R_t) pausing the program with a 1s delay, and any other required pressures are set (T_t) to fulfill multiple variant flow maps over a trajectory (Figure 5d, 5e). Air-flow control is achieved through a set of valves that set initial extrusion inertia (I_t), remain open through the extrusion time, finalize the extrusion accounting for material inertia (F_t), and perform negative pressure to stop the material flow (V_t) (Figure 5d). As a result, the air flow controller time is defined by $A = C + V$, where $C = I_t + T_t - F_t$, and $V = V_t$. It is important to note that the capabilities of pressure allocator, regulator, and controller are processed in quasi-parallel computation through sleep timers over a given trajectory (Figure 5d).

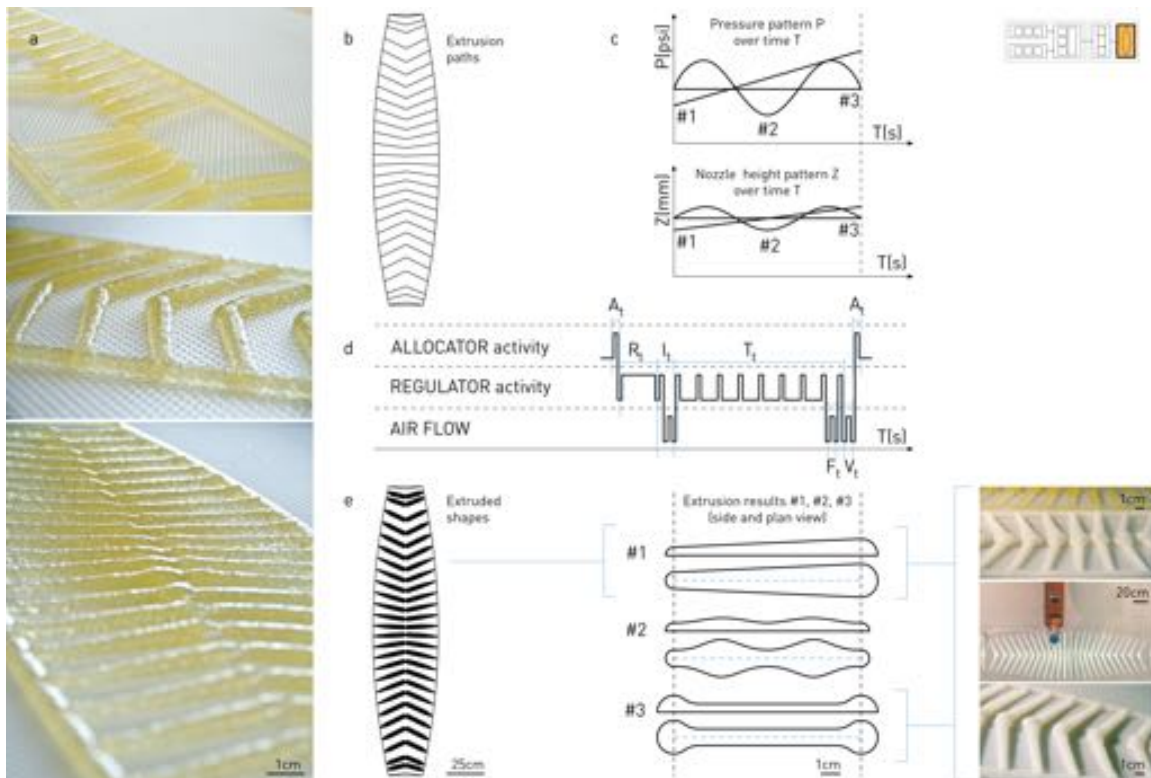


FIGURE 5: (a) Regional-based control is achieved by differentiating extrusion geometries in height and width through variable pressure and motion maps. The examples shown use an hydrogel based material right after being extruded (polysaccharide hydrogel in 9% w/v in 1% acidic solution). (b) Geometrical designs are composed of simple geometries such as points, curves and lines and interpreted by the model into variable extrusion constructs. (c) The extrusions can be incremental (#1), sinusoidal (#2) or follow any other pressure map $P(\text{psi})$ such as #3. They can also follow nozzle height maps $Z(\text{mm})$ in order to result in variable material distribution extrusions. (d) In order to achieve such diversity time-dependent actions are performed in parallel. (e) The resulting extrusion shapes produce a variety of 3D configurations from simple line trajectories.

3.5. The Flow of Time

The flow of time is tied to the flow of pressure. Graphs describing pressure distribution (PSI) and height distribution (Z) over time inform the height and width of regional extrusion geometries (Figure 5c). The minimum and maximum bound of the pressure axis is determined by the empirical material calibration data with each of the

system's nozzles. The graphs describe changes in the time it takes to complete each path trajectory. They are encoded in mathematical formulas where pressure P is dependent on time T ; continuous ($P = a$), incremental ($P = a*T + b$), exponential ($P = T^n$), sinusoidal ($P = a*\sin(b*T + c)$), etc. that the customized firmware, loaded in the pneumatics micro controller, is able to interpret. The encoding is achieved through geometric 2D to 3D mapping. In our case, time and flow mapping instructions transform simple curve primitives (Figure 5a) into 3D extrusion shapes with variable height and width along deposition trajectories (Figure 5e).

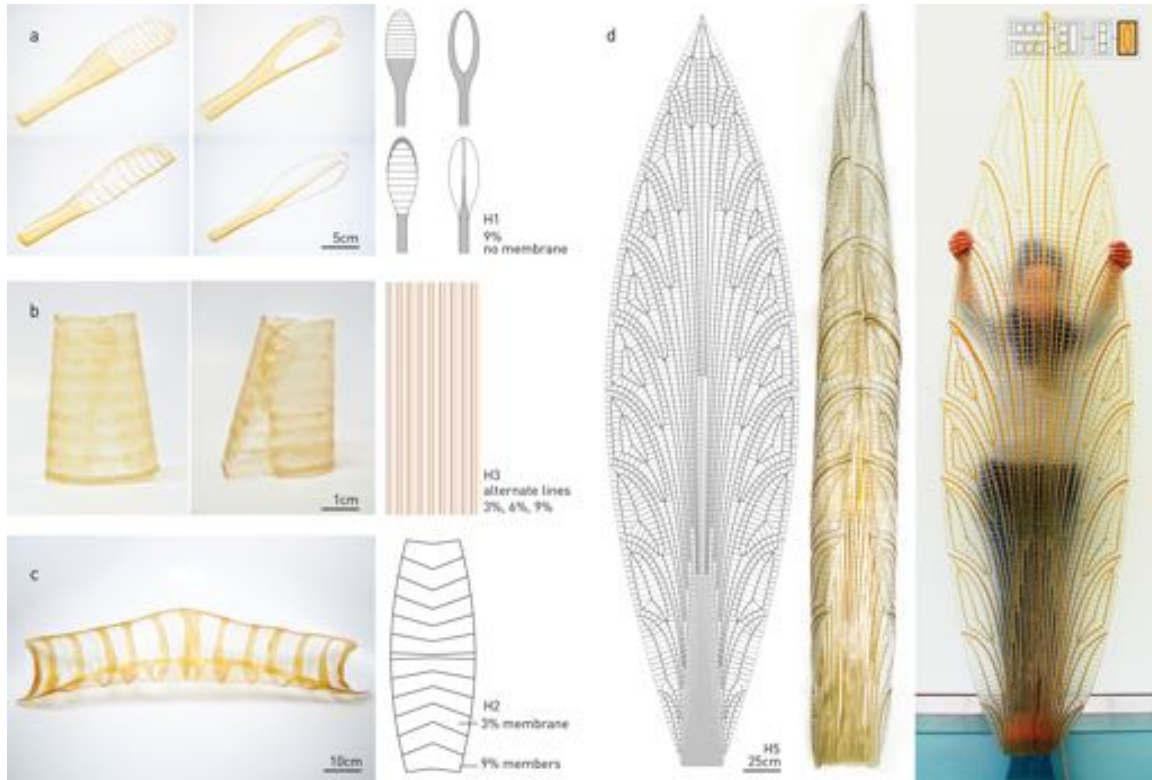


FIGURE 6: (color in Website, black and white in print)

(a) Single material dried extrusions of identical global shapes defined by their boundaries, but with different internal patterns, achieve different global shapes due to varied material distributions. The material used for these examples is a polysaccharide hydrogel. (b) Multi-stiffness polysaccharide hydrogel geometries combining various concentrations (3%, 6% and 9% w/v in mild acidic solution) demonstrate form finding of tubular global shape by means of longitudinal geometric patterning and material shrinkage by water evaporation. (c) A multi-material construct in two levels of hierarchy combines high strength materials at the structural members (9% hydrogel) and low strength materials as infill skin (3% hydrogel) is deposited flat following line trajectories, and form-found due to the shrinkage of the material distributions and its geometric design. (d) A complex large-scale self-supporting construct designed as a cantilevering structure has its curvature defined by geometrical patterning and multi-material deposition in five levels of hierarchy informed by structural stability requirements.

3.6. The Flow of Water

We evaluated materials with viscosities ranging from 500cPs to 50.000cPs at room temperature such as hydrogels, gel-based composites, certain types of clays, organic pastes, resins, polyvinyl alcohols etc. These materials are water-based and undergo slow curing from pastes to solids at room temperature [17]. Global levels of control are achieved by the effect of combined local and regional strategies. Global shapes are revealed in the constructs when the contents of water and solvents of the

materials evaporate into the environment. Single material dried extrusions of the same contour shapes with different internal patterns achieve different global shapes due to varied material distributions (Figure 6a). Multi-material geometries where different wet concentrations are placed side-by-side in a longitudinal manner, achieve significant curvature changes after drying (Figure 6b). Multi-material constructs where structural members are assigned high strength materials and infill surfaces are assigned low strength materials achieve controlled degrees of curvature after drying (Figure 6c). In highly complex large-scale networks, overall curvature is informed by the boundary conditions and the geometrical patterning of internal structures, in addition to multi-material deposition informed by desired structural requirements (Figure 6d).

4. Discussion

The integrated file-to-fabrication workflow presented in this paper is initiated at the designer's CAD software environment and finalized at the DDM technology's operations control. It negotiates shape and material attributes with the DDM technology's mechanical constraints within a single representation and computational environment. The workflow is bidirectional in the sense that it can be implemented for top-down or bottom-up control. Specifically it can process constraints as inputs to generate performance-based fabrication outputs and at the same time it can process performance-based fabrication inputs to generate constraint outputs. When combined, this bidirectional workflow can enable powerful material and site-specific products. In addition, the workflow is designed to control the deposition of both continuous and discontinuous printing modes to support functional gradation. This is achieved through the deposition of materials with variable mechanical properties, through the deposition of single or multiple layers and, finally, through extrusion geometry specifications given by the nozzle shape at the tip.

When generalized, the workflow can support DDM of a wide range of materials, deposition platforms and nozzle designs spanning various application domains characterized by optimal synchronization between the CNC platform and the extrusion system [39]. The multi-material extrusion system (De) can be rapidly mounted on multiple 3-axis CNC platforms (Po) and take advantage of their precise positioning hardware. The attachment to the platform's end-effector can be customized and only requires mechanical means (Figure 3b, 3c). The application of multiple materials and composites provides promising initial validation of the enabling technology and its virtual-to-physical workflow.

Design principles and methods underlying our general model and workflow are defined at the intersection of multiple research areas such as Digital Design, Computer Science, Mechanical Engineering and Materials Science and Engineering. This rich plexus of knowledge contributes to the generation of complex CAD tools, techniques and technologies tailored to provide LSHD for complex 3D designs.

4.1. Results

The integrated system and workflow can achieve a continuous and seamless multi-dimensional design-to-fabrication data flow (Figure 1). Based on system invariant constraints and decision-driven variant input sets (Figure 2), a hierarchical model is implemented operating at three levels of resolution defined as local, regional and global.

Basic geometric primitives are associated with diverse materials and extrusion shapes where; local refers to the way material is deposited in gradients and layering patterns (Figure 4), regional refers to the 3D shapes in which material can be extruded (Figure 5), and global refers to the topologic effects of material organization, combining both local and regional strategies (Figure 6). Based on these domain definitions interrelated meta-data is encoded into transmission instructions that synchronize motion and deposition platforms (Figure 3) to produce heterogeneous structured objects with viscous water-based materials. It is important to note that 3D constructs and complex material organization will emerge, not by direct 3D modeling, but by meta-data informing the manufacturing process with its different motions, variable pressures and diverse material compositions to deposit (Figure 5, 6).

Local

By fine-tuning mechanical property gradients and layered compositions of multi-material extrusions we achieve local hierarchical control. Figure 4a illustrates hierarchical deposition. Material distribution patterns and resulting dry constructs are shown in cross section and. In Figure 4b different concentrations of polysaccharide hydrogel in mild acidic solutions are employed to generate a gradient of materials with varying degrees of stiffness, viscosity and opacity. Unique mechanical behaviors emerge along the structures by associating and assigning these materials to the designed geometries.

Regional

Regional-based control is achieved by differentiating extrusion geometries in height and width through variable pressure and motion. The examples illustrated in Figure 5a are of hydrogel based material immediately following its extrusion. Figure 5b demonstrates designs composed of simple geometries such as points; curves and lines interpreted by the model into variable extrusion constructs, as shown in Figure 5a. The extrusions can be incremental (#1), sinusoidal (#2) or follow other pressure maps $P(\text{psi})$ such as given in #3. They can also follow nozzle height maps $Z(\text{mm})$ in order to achieve variable material distribution (Figure 5c). Variations in mechanical and optical properties are enabled by time-dependent actions performed in parallel. A data allocator reads the instructions first, based on allocation time (A_t). A regulator then sets initial pressure units (R_t) and any other required pressures (T_t) implementing the desired flow maps over a given trajectory. Airflow control is achieved through a set of valves that require time to set initial extrusion (I_t), stay open through the extrusion time, finalize the extrusion accounting for material inertia (F_t), and apply negative pressure to stop the material flow (V_t) (Figure 5d). The resulting extrusion shapes produce a variety of 3D configurations from simple line trajectories. In the example, the lines from Figure 5b are deposited in type #1 extrusions using a hydrogel-cellulose composite (Figure 5e).

Global

Global-based control is achieved by combining local and regional deposition strategies within global shapes. Figure 6 shows heterogeneously structured multi-functional objects. We deposit different materials with different structural capacities at different levels of hierarchy ranging from one to five. The material distribution geometries and material properties defined for each deposition trajectory inform the final global shape. For instance, in Figure 6a, the same global shape is structured with different internal patterns and the cured constructs display corresponding global shapes induced by

the shrinking forces of each pattern. In Figure 6b, water-based gels with different concentrations are deposited in a plane, to produce a dried tubular shape. In Figure 6c, tubular structural elements and surface elements are designed with two materials deposited in a spiral pattern; a stiff rubber-like gel and a light film-forming gel. We used incremental pressure maps to deposit higher amounts of material in the center of the spine trajectories, which induced a controlled deformation pattern providing structural inertia to the construct. In Figure 6d, a large-scale structure is extruded with five levels of hierarchy as shown in Figure 4a. Its structural pattern is inspired by insect wing or leaf venation structures, and its final global shape demonstrates controlled folding into a robust and lightweight cantilever beam configuration.

4.2. Future Work

This paper introduces a novel workflow for direct additive manufacturing of multifunctional heterogeneously structured objects. The workflow enables the design and digital fabrication of structural parts made of water-based materials characterized by spatial and material complexity. At its core the workflow integrates virtual data with physical data enabling real time calibration of data and material flow.

Through the implementation of this workflow we have demonstrated the design and direct additive manufacturing of structurally patterned lightweight shells spanning overall distances of 10-feet, with a minimum amount of support, and thin cross-sections (Figure 6). For future applications we plan to explore additive manufacturing of solid structures constructed out of a wider range of structural materials. In addition we plan to continue our research into AM of water-based viscous pastes, with relatively fast cure times or that are fused at the nozzle. Based on the results we will compare the strengths and limitations of our workflow and platform to other alternative approaches.

In terms of local structural controls we have demonstrated our ability to additively manufacture 3D objects characterized by high levels of control over local, regional, and global structures at the meso and macro levels. Future research will focus on enhancing material complexity at micro and nano scales combining micro layering of specific material structures and properties to produce high resolution composites inspired by natural structures such as nacre or silk [17].

In particular we are excited by the possibility of reversing the design workflow to enable formal iterations to the virtual model. This feature will aid closing the loop characteristic of the file-to-factory paradigm and will promote a factory-to-file methodology thereby further refining the workflow as feedback-enabled. Such feedback positive workflow will incorporate interrogative methods such as environment-specific and performance-based predictive modeling [34]. Furthermore, the effect of temperature, humidity, light or airflow can be modeled at the global level of resolution thereby informing both local and regional features. Global shape outcomes could then be visualized in the virtual model for informed design decision-making prior to final fabrication. Such closed loop fabrication workflows will contribute not only to a substantial improvement of virtual-to-physical flow field computation, but will also offer insight into the way in which CAD platforms for HOM are designed and implemented.

Acknowledgments

This research was primarily sponsored by the Mediated Matter research group at the MIT Media Lab. Ideas, methods, products and techniques were developed to support an ongoing group project and research platform focusing on large-scale biodegradable additive manufacturing commissioned by the TBA- 21 Academy (Thyssen-Bornemisza Art Contemporary). The work was supported in part by the U. S. Army Research Laboratory and the U. S. Army Research Office through the Institute for Soldier Nanotechnologies, under contract number W911NF-13-D-0001. The authors would like to thank Dr. Javier Fernandez and Dr. James Weaver from the Wyss Institute at Harvard University, for their guidance and support in the material science aspects of the project. In addition, we wish to thank our colleagues from the MIT Media Lab for their support of this project, including Markus Kayser, William Patrick, John Klein, Chikara Inamura, Steven Keating, and our undergraduate researcher Daniel Lizardo.

References

- [1] Vincent J., Structural Biomaterials, Princeton University Press, 2012 .
- [2] Gibson L. J. and Ashby M. F., Cellular solids: structure and properties, Cambridge University Press, 1999.
- [3] Vincent J., Bogatyreva O. A., et al., Biomimetics: its practice and theory, Journal of the Royal Society Interface, 2006; 3:471-482.
- [4] Oxman N., Material-Based Design Computation, Massachusetts Institute of Technology, 2010.
- [5] Oxman N., Structuring materiality: design fabrication of heterogeneous materials, Architectural Design, 2010; 80:78-85.
- [6] Oxman N., Variable property rapid prototyping, Virtual and Physical Prototyping, 2011; 6:3-31.
- [7] Duro-Royo J., Zolotovskiy K., Mogas-Soldevila L., Varshney S., Oxman N., Boyce M.C., Ortiz C., MetaMesh: A hierarchical computational model for design and fabrication of biomimetic armor surfaces, Computer-Aided Design, Elsevier, 2014; in press.
- [8] Biswas A., Fenves J.S., Shapiro V., Representation of heterogeneous material properties in the Core Product Model. Engineering with Computers 2008; 24:43-58.
- [9] Shapiro V., Tsukanov I., et al., Modeling and analysis of objects having heterogeneous material properties, Google Patents, 2004.
- [10] Shapiro, V., Tsukanov I., et al., Geometric issues in computer aided design/computer aided engineering integration, Journal of Computing and Information Science in Engineering, 2011; 11:021005.
- [11] Chiu W. and Yu K., Direct digital manufacturing of three-dimensional functionally graded material objects, Computer-Aided Design, 2008; 40:1080- 1093.
- [12] Biswas A., Shapiro V., Heterogeneous material modeling with distance fields. Computer Aided Geometric Design 2004; 21:215-242.
- [13] Vidimce K., Wang S., Ragan-Kelley J., Matusik W., OpenFab: A Programmable Pipeline for Multi-Material Fabrication. SIGGRAPH Conference Proceedings 2013; 32:1-12.

- [14] Kou, X.Y., Tan S. T., Heterogeneous Object Modeling: A review, *Computer-Aided Design*, 2013; 39:284-301.
- [15] Hon K.K.B., *Additive Manufacturing Technologies: Rapid Prototyping to Direct Digital Manufacturing*, Springer, 2010.
- [16] Gibson I., Rosen D. W., et al., *Direct digital manufacturing. Additive manufacturing technologies*, Springer, 2010; 363-384.
- [17] Mogas-Soldevila L., Duro-Royo J., Oxman N., *Water-based Robotic Fabrication: Large-Scale Additive Manufacturing of Functionally-Graded Hydrogel Composites via Multi-Chamber Extrusion, 3D Printing and Additive Manufacturing*, 2014; 1:1-11.
- [18] Kieback B., Neubrand A., Riedel H. Processing techniques for functionally graded materials. *Materials Science and Engineering* 2003; 362:81-106.
- [19] Malone E. and Lipson H., Multi-material freeform fabrication of active systems. *ASME 2008 9th Biennial Conference on Engineering Systems Design and Analysis*, American Society of Mechanical Engineers, 2008.
- [20] Hiller J. and Lipson H., Design and analysis of digital materials for physical 3D voxel printing, *Rapid Prototyping Journal*, 2009; 15:137-149.
- [21] Hiller J. and Lipson H., Tunable digital material properties for 3D voxel printers, *Rapid Prototyping Journal* 2010; 16:241-247.
- [22] Weiss L., Merz R., et al., Shape deposition manufacturing of heterogeneous structures, *Journal of Manufacturing Systems*, 1997; 16:239-248.
- [23] Kumar V. and Dutta D., An approach to modeling and representation of heterogeneous objects, *Journal of Mechanical Design*, 1998; 120:659-667.
- [24] Samanta K. and Koc B., Feature-based design and material blending for free-form heterogeneous object modeling, *Computer-Aided Design*, 2005; 37:287-305.
- [25] Siu Y.K. and Tan S.T., Modeling the material grading and structures of heterogeneous objects for layered manufacturing, *Computer-Aided Design*, 2002; 34:705-716.
- [26] Kou X. and Tan S., A hierarchical representation for heterogeneous object modeling, *Computer-Aided Design*, 2005; 37:307-319.
- [27] Biswas A., Shapiro V., et al., Heterogeneous material modeling with distance fields, *Computer Aided Geometric Design*, 2004; 21:215-242.
- [28] Chen J. and Shapiro V., Optimization of continuous heterogeneous models, *Heterogeneous objects modeling and applications*, Springer: 193-213, 2008.
- [29] Pratt M.J., Modeling of Material Property Variation for Layered Manufacturing. In: Cipolla R. and Martin R., editors. *The Mathematics of Surfaces IX*, Springer, 2000, p.486-500.
- [30] Oosterhuis K., *File to Factory and Real Time Behavior in Architecture, Fabrication: Examining the Digital Practice of Architecture*. Proceedings of Conference of the AIA Technology in Architectural Practice Knowledge Community, Cambridge/Ontario, 2004.
- [31] Afify H. M. and Elghaffar Z. A. A., *Advanced Digital Manufacturing Techniques (CAM) in Architecture Authors*, Proceedings of the 3rd International ASCAAD Conference, 2007.
- [32] Scheurer F., Materializing complexity, *Architectural Design*, 2010; 80:86-93.
- [33] Oosterhuis K., Bier H., Aalbers C., Boer S., *File-to-Factory and Real-Time Behaviour in ONL-Architecture*. *AIA/ACADIA Fabrication: Examining the Digital*

Practice of Architecture, 2007, Cambridge and Toronto, Ontario, University of Waterloo School of Architecture Press, p.294-305.

[34] Sheil B., De-Fabricating Protoarchitecture. In: Stacey M., editor. Prototyping Architecture Conference, 2013, Building Centre Trust, London, p.372- 390.

[35] Sass L. and Oxman R., Materializing design: the implications of rapid prototyping in digital design, *Design Studies*, 2006; 27:325-355.

[36] Chang, C., Direct slicing and G-code contour for rapid prototyping machine of UV resin spray using PowerSOLUTION macro commands, *The International Journal of Advanced Manufacturing Technology*, 2004; 23:358-365.

[37] Farouki R. T., Manjunathaiah J., et al., G codes for the specification of Pythagorean-hodograph tool paths and associated feedrate functions on open-architecture CNC machines, *International Journal of Machine Tools and Manufacture*, 1999; 39:123-142.

[38] McNeel R., Grasshopper generative modeling for Rhino, Computer software (2011b), <http://www.grasshopper3d.com>, 2010.

[39] Duro Royo J., Mogas Soldevila L. and Oxman N., Methods and Apparatus for Integrated Large Scale Robotic Fabrication of Functionally Graded Materials and Structures, US provisional patent (M.I.T. Case No. 17388T), 2014.

[40] Sun W., Starly B., Nam J., Darling A., Bio-CAD modeling and its applications in computer-aided tissue engineering. *Computer-Aided Design*, 2005; 37:1097-1114.

[41] Fryazinov O., Pasko A., Reliable detection and separation of components for solid objects defined with scalar fields, *Computer-Aided Design*, 2015; 58:43-50.

[42] Takayama K., Sorkine-Hornung O., Nealen A., Igarashi T., Volumetric Modeling with Diffusion Surfaces, *Proceedings of ACM SIGGRAPH ASIA 2010*, New York, 2010; 180:1-7.